Process Biochemistry 108 (2021) 80–89

Contents lists available at ScienceDirect

Process Biochemistry

journal homepage: www.elsevier.com/locate/procbio

Electrochemical catechol biosensor based on β-cyclodextrin capped gold nanoparticles and inhibition effect of ibuprofen

Beste Kapan [a], Sevinc Kurbanoglu [b], Emren Nalbant Esenturk [a], Saniye Soylemez [c,*], Levent Toppare [a,d,e,f,**]

[a] Department of Chemistry, Middle East Technical University, Ankara, 06800, Turkey
[b] Department of Analytical Chemistry, Faculty of Pharmacy, Ankara University, 06560, Ankara, Turkey
[c] Department of Chemistry, Ordu University, Ordu, 52200, Turkey
[d] Department of Biotechnology, Middle East Technical University, Ankara, 06800, Turkey
[e] Department of Polymer Science and Technology, Middle East Technical University, Ankara, 06800, Turkey
[f] The Center for Solar Energy Research and Application (GUNAM), Middle East Technical University, Ankara, 06800, Turkey

ARTICLE INFO

Keywords:
Catechol detection
Enzyme inhibition
β cyclodextrin
Gold nanoparticles
Ibuprofen
Tyrosinase

ABSTRACT

Herein, β-cyclodextrin-capped gold nanoparticle surface designed for tyrosinase (Tyr)-based nanosensor is proposed and demonstrated. Integration of the β-cyclodextrin-capped gold nanoparticles on graphite electrode surface was achieved via drop-casting method, Tyr was immobilized on the modified electrode and then used as drug inhibition platform with catechol as the substrate. All optimization studies that affect biosensor response were conducted, and catechol was detected in the linear range of 1.56 μM-25μM catechol concentration with a limit of detection of 0.42 μM and sensitivity of 2.094 $\mu A.\mu M^{-1}.\ cm^{-2}$. Tyr inhibition was followed with ibuprofen drug active compound with a 15 min incubation time, and the I_{50} value was found as 213 μM. The sensor is the first in the literature to use an electrochemical method for β-cyclodextrin-capped gold nanoparticles based Tyr biosensor and ibuprofen inhibition. This sensor presents an easy fabrication method, excellent sensor properties, and ibuprofen inhibition capabilities. As a result, it is proposed that the designed sensor is an ideal marker for detecting Tyr inhibition using electrochemical methods and an ibuprofen-based cosmetic cream formulation could be a viable option in the cosmetic market.

1. Introduction

Biosensors and their applications in medical science, cosmetics, environmental analysis, and other fields, such as early-stage detection of significant biomarkers and rapid detection of analytes, are critical. Because of its wide range of importance, research in this area is undoubtedly expanding. This has resulted in the development of sensitive and powerful analytical tools that employ the biological sensing element as a biosensor. Enzyme-based biosensors, in particular, are preferred sensor systems over others such as immunosensors, genosensors, and cell-based sensors [1–3]. The enzyme immobilization stage is critical in the development of electrochemical enzyme-based biosensors [4]. Enzyme-based biosensors have been built using a variety of materials ranging from nanomaterials to polymers. Nanomaterials are useful in catalysis, mechanics, optics, cosmetics, physics, and biomedical sciences [5]. The construction of biosensors is an important application of nanomaterials since they have great properties such as high surface-to-volume ratio, stability, and biocompatibility, allowing for great architecture for biomolecule immobilization [6,7].

Efficient biomolecule immobilization methods on the transducer surface employ a variety of approaches, including hydrogen bonding, electrostatic and hydrophobic interactions, and π–π stacking. Nanomaterials, coated with natural or synthetic polymers like polyaniline, gelatin, chitosan, and montmorillonite offer, an excellent architecture for the immobilization of biomolecules [8–10]. Gold nanoparticles (AuNPs) have received great attention in recent years due to their excellent conductivity and superior catalytic activity [11–13]. So far, they have demonstrated promising results in the development of biosensors due to their distinct chemical and physical properties [12–15]. Furthermore, because cyclodextrins (CDs) have both hydrophilic and

* Corresponding author at: Ordu University, Department of Chemistry, 52200, Ordu, Turkey.
** Corresponding author at: Middle East Technical University, Department of Chemistry, 06800, Ankara, Turkey.
E-mail addresses: saniyesoylemez@odu.edu.tr (S. Soylemez), toppare@metu.edu.tr (L. Toppare).

https://doi.org/10.1016/j.procbio.2021.06.004
Received 19 January 2021; Received in revised form 1 June 2021; Accepted 4 June 2021
Available online 8 June 2021
1359-5113/© 2021 Published by Elsevier Ltd.

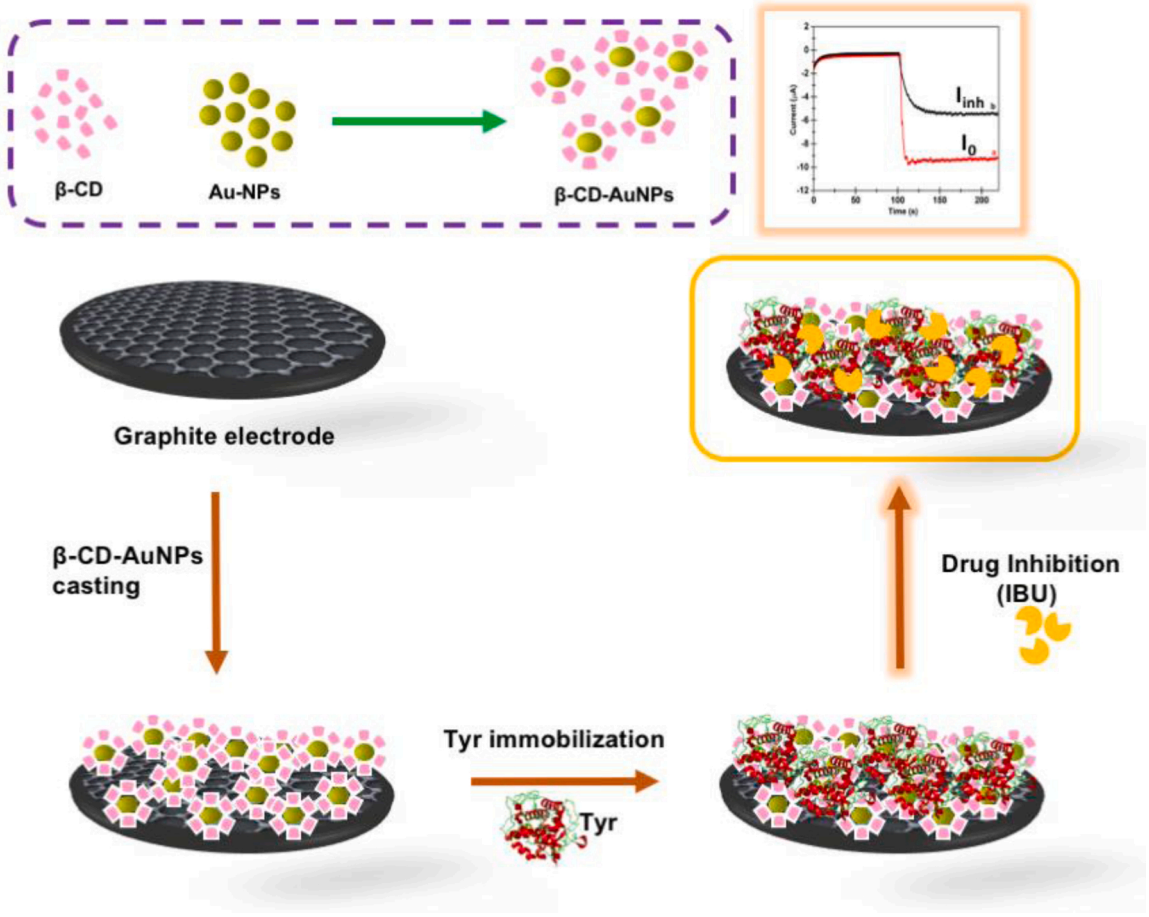

Scheme 1. Schematic representation of the fabrication of the nanobiosensor.

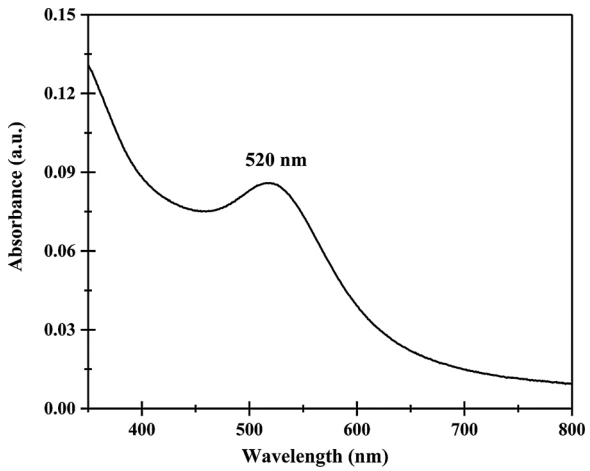

Fig. 1. UV–vis result of theβ-CD-AuNPs.

hydrophobic properties, they can form new supramolecular complexes, which has sparked a lot of interest in a variety of chemistry applications [16].

To the best of our knowledge, the direct synthesis of CD-modified AuNPs from the reaction between $HAuCl_4$ with pristine β-cyclodextrin has never been reported for Tyrosinase (Tyr) based biosensors and drug inhibition studies. Since β-cyclodextrin based surfaces offer stabilized surfaces in the design of enzymatic biosensors via formation of supramolecular complexes and host-guest associations between the cyclic oligosaccharides and the enzyme, their use in enzyme inhibition studies is also vital. Moreover, suggesting new drugs for an alternative Tyr inhibitor is another crucial issue in cosmetics. Tyr enzyme is responsible for melanin formation, and excess melanin formation causes many dermatological problems. Tyr inhibition can be used to inhibit melanin biosynthesis. Arbutin, kojic acid-based cosmetic products on the market, are less effective in standard topical treatments for hyperpigmentation; thus, new inhibitors are constantly being researched. Ibuprofen, (IBU, (RS)-2-[4-(2-methylpropyl)phenyl]propanoic acid) belongs to the nonsteroidal anti-inflammatory drug family. It is an important drug used to treat pain, fever, and inflammation. It can be taken orally or intravenously [17,18]. According to the literature, IBU may also inhibit the Tyr enzyme, and this inhibition was monitored using spectrophotometric techniques [19–21]. There is no electrochemical method to follow this inhibition, which is the main focus of our research. Because of their role in dermal melanin production, tyr inhibitors are preferred as whitening or anti-hyperpigmentation agents, implying that an alternative whitening agent is critical for the cosmetic industry.

Hence, in this study, we synthesized and characterized β-cyclodextrin capped gold nanoparticles (β-CD-AuNPs) and used it for the construction of a novel nanobiosensor for Tyr immobilization (Scheme 1). The designed biosensor was then further used for Tyr inhibition via IBU drug active compound by monitoring the decrease in catechol response. In this study, the inhibition of Tyr due to the decrease in catechol response in the presence of IBU was monitored using chronoamperometry method. The effect of biosensor parameters on biosensor response, inhibition time, and inhibitor concentration dependence were also tested and optimized.

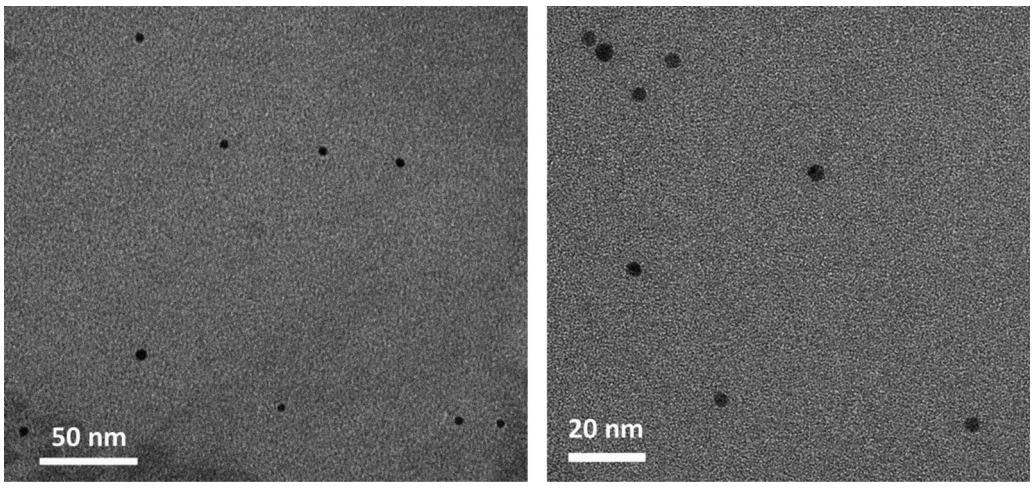

Fig. 2. TEM images ofβ-CD-AuNPs at different magnifications.

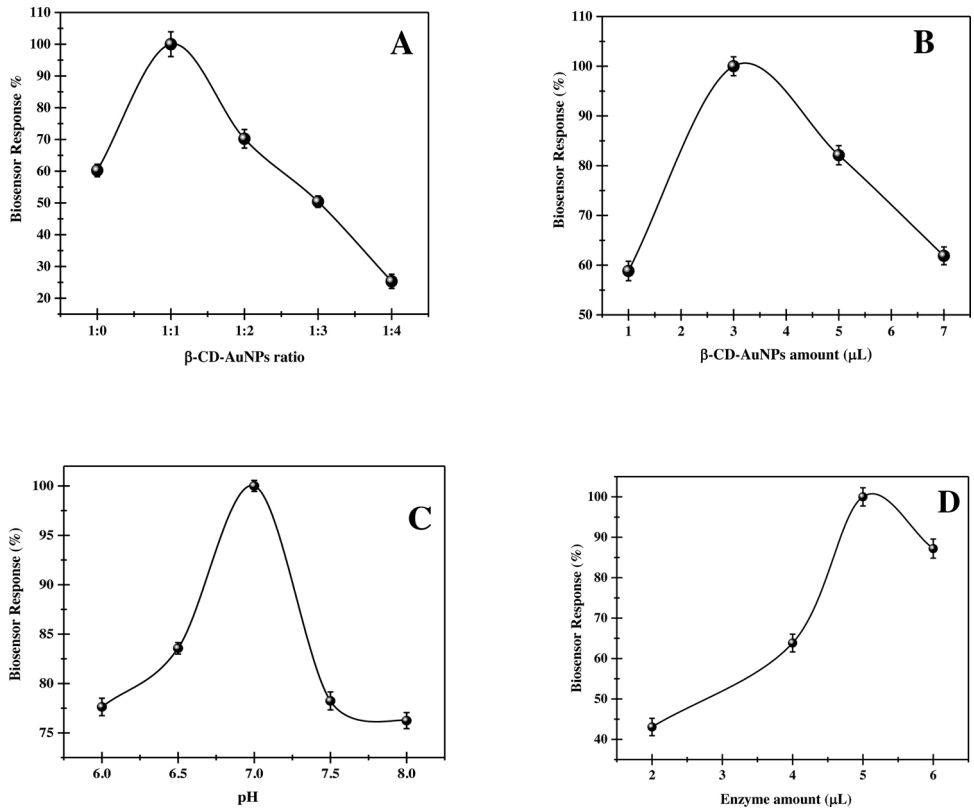

Fig. 3. Optimization of (A) the ratio of β-CD-AuNPs (B) the amounts of β-CD-AuNPs (C) pH and (D) Try amount. Experimental conditions: a working potential of −200 mV in 50 mM phosphate buffer at pH 7.0.

2. Experimental

2.1. Apparatus and reagents

PalmSens electrochemical analyzer with a software package PSTrace Version 5.8 was equipped for electrochemical experiments. A three-electrode system was utilized in amperometric measurements consisting of a graphite rod electrode (GE, 3.05 mm diameter), Pt wire, and silver wire pseudo electrode as the working, counter, and reference electrodes, respectively. Each amperometric measurement was repeated three times, and the average was recorded and expressed as ± SD. All measurements were taken at room temperature.

Each modified surface morphologies of sensor layers were investigated using JEOL JSM-6400 models Scanning Electron Microscopy (SEM). Atomic force microscopy (AFM) analysis was carried out using Veeco Multimode V AS-130 (“J”). Transmission electron microscopy images (TEM) were obtained using FEITecnaiG2 Spirit BioTwinCTEM Microscope. The average hydrodynamic size of nanoparticles was obtained by the DLS technique using MALVERN Instruments.

Mushroom Tyrosinase (25 KU, lyophilized powder, the activity of 7164 Units per mg of solid), Pyrocatechol, approx. 99 %, glutaraldehyde 50 wt. % in H_2O as the cross linking agent, sodium phosphate monobasic (H_2NaO_4P), β-cyclodextrin ($C_{42}H_{70}O_{35}$), ibuprofen (IBU), and $HAuCl_4$ were purchased from Sigma-Aldrich (St. Louis, MO, USA). Sodium

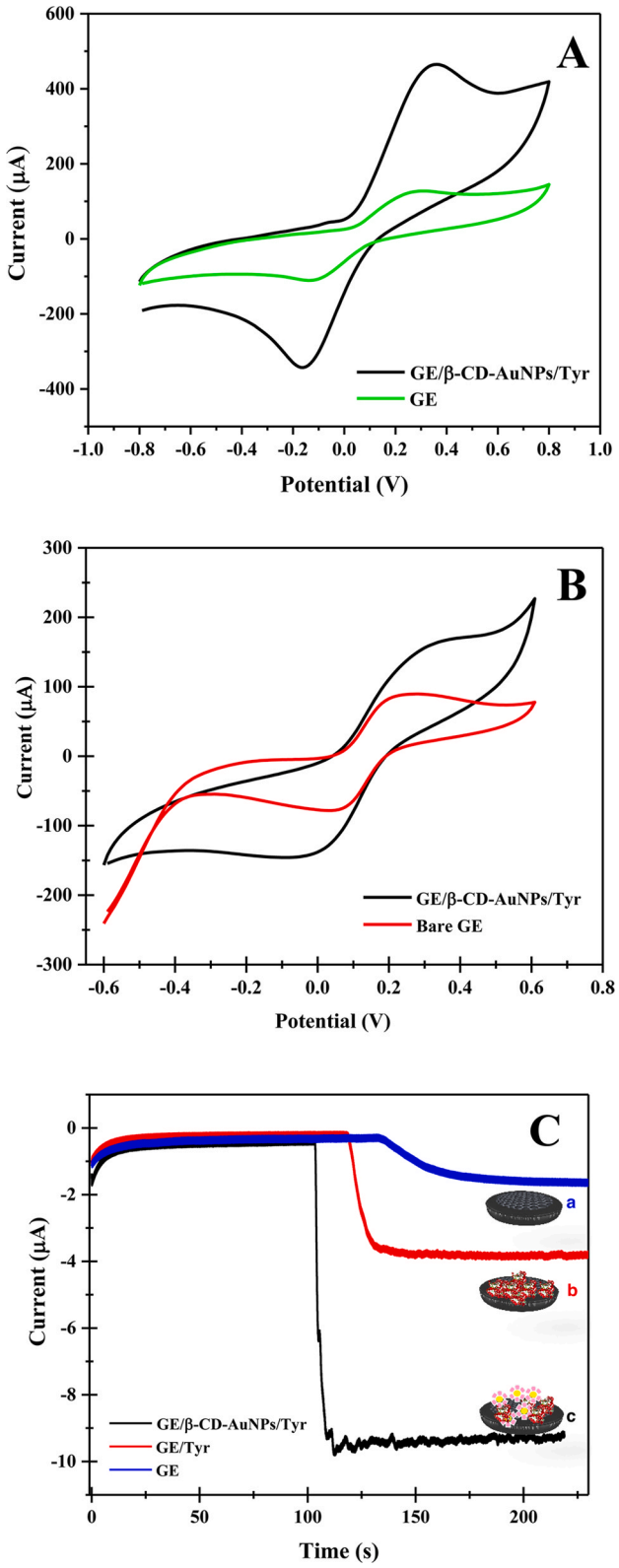

Fig. 4. (A) Cyclic voltammograms of bare graphite electrode (GE) and GE/β-CD-AuNPs/Tyr in the presence of 1.25 mM catechol at a scan rate of 100 mV/s in 50 mM phosphate buffer at pH 7.0 (B) cyclic voltammograms of bare graphite electrode (GE) and GE/β-CD-AuNPs/Tyr in 5.0 mM $K_3[Fe(CN)_6]/K_4[Fe(CN)_6]$ containing 50 mM phosphate buffer at pH 7.0 (C) amperometric responses of (a) GE (b) GE/Tyr (c) GE/β-CD-AuNPs/Tyr.

phosphate dibasic ($Na_2HPO_4.2H_2O$), and sodium hydroxide (NaOH) were purchased from (Merck KGaA, Darmstadt, Germany). All chemicals were of analytical grade unless otherwise stated. The aqueous solutions were prepared using deionized (DI) water (resistivity > 18 MΩ, PURELAB Option-Q, ELGA).

2.2. Synthesis of β-cyclodextrin-capped gold nanoparticles

The reduction of $HAuCl_4$ with β-CD in the alkaline aqueous solution method was used to synthesize β-CD-capped AuNPs based on the previously reported method [22]. 0.0396 *g* of β-cyclodextrin was dissolved in 4.93 mL deionized water and thoroughly shaken. After β-cyclodextrin was completely dissolved, 20 μL of $HAuCl_4$ (10 mM) were added to this solution. After 2 min, NaOH (1.0 M) was added to the solution to obtain a pH of between 9 and 10 (~9.83). After vigorous shaking, the solution was kept at 50 °C for 20 min without stirring. Finally, the transformation of the solution's color from colorless to pink indicates the formation of β-cyclodextrin-capped AuNPs. The synthesized AuNPs were purified by centrifugation (at 10000 rpm for 15 min) and re-dispersed NPs in fresh DI water.

2.3. Preparation of GE/β-CD-AuNPs /Tyr nanobiosensor

Graphite rods were polished with emery paper and washed with distilled water. Then, a 5 μL mixture of freshly prepared β-CD-AuNPs (1:1 diluted with deionized (DI) water) and Tyr enzyme was immobilized onto the cleaned graphite rods. After 2 min, 5 μL of 1 % glutaraldehyde solution were spread over the GE/ β-CD-AuNPs /Tyr surface. Well-prepared graphite electrodes were left to dry for 2 h before conducting the sensing experiments at room temperature.

2.4. Catechol detection using GE/ β-CD-AuNPs /Tyr nanobiosensor

Amperometric measurements were performed at room temperature with stirring in the reaction medium containing 10 mL buffer solution (50 mM, pH 7.0) at room temperature under stirring by applying −200 mV constant potential. After each measurement, a clean buffer was used to replace the used one. After waiting for the current to stabilize, 25 μM catechol was added to the reaction medium to conduct optimization studies. The difference in current produced an electrochemical biosensing response.

2.5. Inhibition studies with ibuprofen

After preparation and optimization of GE/β-CD-AuNPs /Tyr nanobiosensor, Tyr inhibition by IBU was examined. 0.3 mM stock solution of IBU was prepared in phosphate buffer and diluted with phosphate buffer to desired concentrations. First, catechol measurement was taken once to stimulate all well-prepared electrodes. The signal taken from all of the initial measurements was recorded as Io for each electrode separately. After carefully washing the electrodes with distilled water, they were immersed into a tube containing different concentrations of IBU solutions for different inhibition times to inhibition of Tyr by IBU. Following this, catechol measurements were retaken from each immersed biosensor, and relative inhibition of Tyr by IBU was monitored via the decrease in catechol response.

3. Results and discussion

3.1. Characterization of β-CD-AuNPs

In order to characterize the synthesized β-CD-AuNPs, UV visible and TEM analyses were performed. Fig. 1 shows the UV–vis spectra of gold nanoparticles prepared using β-CD in alkaline aqueous solution by reducing $HAuCl_4$. As shown in the Fig. 1, the characteristic pink absorption band located at 520 nm validates an adequate formation of

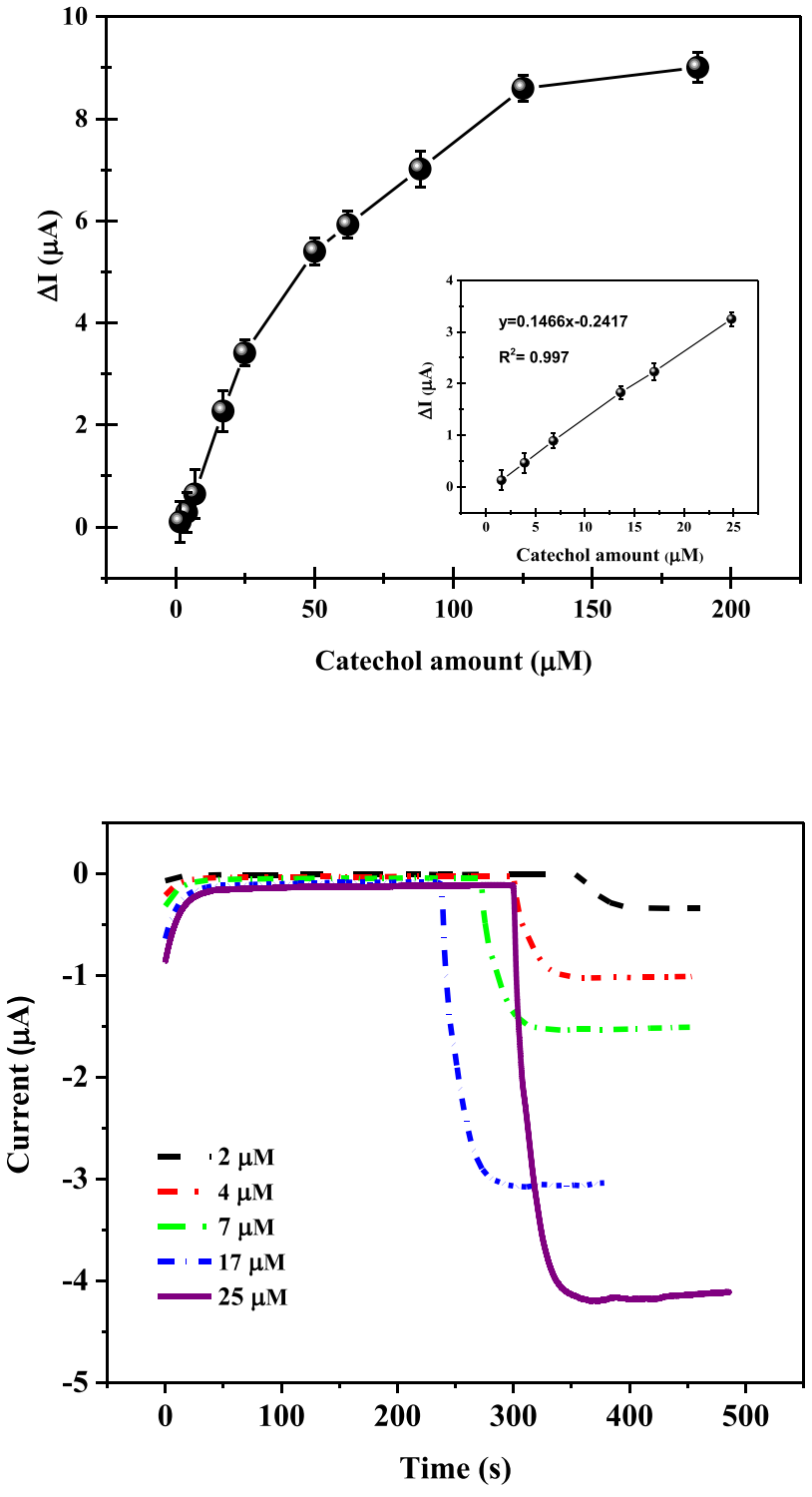

Fig. 5. (A) Analytical calibration of the GE/β-CD-AuNPs /Tyrnanobiosensor (B) Different concentrations of catechol responses using GE/β-CD-AuNPs /Tyr nanobiosensor. Experimental conditions: a working potential of −200 mV in 50 mM phosphate buffer at pH 7.0.

β-CD-AuNPs. Hence, the results are in good correlation with the previous literature examples [22,23].

Fig. 2 presents the TEM images of β-CD-AuNPs at different magnifications. The images reveal that the use of β-CD as the capping agent yielded spherical NPs with 5 ± 0.4 nm size. Moreover, the TEM analysis clearly shows that the synthesized nanoparticles are very uniform with narrow size distribution (Figure S1).

3.2. Optimization studies and electrochemical characterizations of GE/β-CD-AuNPs /Tyr nanobiosensor

The suggested GE/β-CD-AuNPs /Tyr nanobiosensor was optimized in terms of the amount of β-CD-AuNPs, the ratio of β-CD-AuNPs, pH and Tyr amount using chronoamperometric responses for 25 μM catechol within a working potential of −200 mV. First, β-CD-AuNPs were mixed with DI water to observe the dilution effect on biosensing response, and

Table 1
Comparison of some selected Tyr-based detection platforms for catechol using graphite electrode.

Sensors	Linear range	LOD	Sensitivity	Refs.
GE/MWCNTs-TiO_2/Tyr	0.2 - 2.7 mM	0.014 μM	85.79 mA.M^{-1}	[44]
GE/Nafion/Tyr	50–1000 μM	0.015 μM	9.83 nA.μM^{-1}	[45]
GE/Eastman AQ/ Tyr	0.05–150 μM	0.030 μM	2.91 nA.μM^{-1}	[45]
GE/PPy/ AgNPsTyr	0.001- 0.015 mM	0.47 μM	13.66 μM^{-1} cm^{-2}	[46]
GE/PPyNT/ $SrCuO_2$/Tyr	1-50 μM	0.15 μM	15.60 μA. μM^{-1}. cm^{-2}	[47]
GE/GNRs/ AgNPs/ Tyr	2-2300 μM	0.03 μM	6.28 μA.mM^{-1}. cm^{-2}	[48]
GE/β-CD-AuNPs/Tyr	**1.56 μM-25μM**	**0.42 μM**	**2.094 μA. μM^{-1}. cm^{-2}**	**Our work**

MWNT: multiwalled nanotubes; GE: Graphite Electrode; PPyNT:polypyrrole nanotubes; $SrCuO_2$:strontium copper oxide micro-seeds; GNRs: graphene nanoribbon.

the ratios of 1:0, 1:1, 1:2, 1:3 (β-CD-AuNPs:DI water) were examined. The optimum response was obtained using the 1:1 ratio, as shown in Fig. 3A. For optimization of β-CD-AuNPs amount, different amounts of 1:1 β-CD-AuNPs, varying between 1 μL and 7 μL, were cast onto the surface of GE and checked against 25 μM catechol response. Hence, using 3 μL β-CD-AuNPs, the highest catechol response was obtained, and it was used for further experiments (Fig. 3B). After optimizing the amounts and ratio of β-CD-AuNPs, the pH of the working buffer was varied between 6.0 and 8.0. Using phosphate buffer with pH 7.0, reliable responses were obtained as seen in Fig. 3C. Lastly, enzyme loading experiments were performed using different units of Tyr (286.56 U to 859.68 U). When a higher amount of Tyr was immobilized, an enzyme leak from the electrode surface was observed in correlation with the inadequate response of the related biosensor. Hence, the enzyme amount of 716.4 U was the optimum and it was used for further studies (Fig. 3D).

Electrochemical properties of the designed GE/ β-CD-AuNPs /Tyr nanobiosensor were observed by cyclic voltammetry (CV) technique in 1.25 mM catechol and in 5.0 mM $K_3[Fe(CN)_6]/K_4[Fe(CN)_6]$ containing 0.10 M KCl. This complex is a well-known redox marker for enhancing the biosensor responses upon modification. As seen from Fig. 4A, an increase in the biosensor's surface area increases, the redox couple's response. As a further improvement, the biosensor's effective surface area after modification was also calculated using Fig. 4A. The electrochemical active surface area of the electrode was found by substituting the valve of the slope of the peak current versus the scan rate plot in Randles–Sevcik, where I_p is the peak current (μA), n refers to the electrons involved in the redox reaction, A is the effective surface area of the electrode (cm^2), υ is the scan rate ($V.s^{-1}$), D is the diffusion coefficient ($cm^2.s^{-1}$), and C is the concentration of $[Fe(CN)_6]^{3-/4-}$ (mol. cm^{-3}) [24–26].

$$I_p = (2.69 \times 10^5)\, n^{3/2}\, A\, D^{1/2}\, \nu^{1/2}\, C_0$$

From this equation, the biosensor's effective surface area was calculated as 0.141 cm^2 which is 2.11 times greater than the valve for the bare electrode.

From Fig. 4B, it is clearly seen that catechol had the highest reduction response at −200 mV; therefore, further experiments were conducted by applying −200 mV in amperometry. Hence, amperometric responses for step-by-step modification (Fig. 4B) also indicate that a modification of the GE's surface with β-CD-AuNPs improved the catechol response.

3.3. Analytical characterization of GE/β-CD-AuNPs /Tyr nanobiosensor

Under optimized conditions, analytical characterization of chronoamperometric catechol detection was performed using GE/β-CD-AuNPs/Tyr nanobiosensor. The linear range was obtained between 1.56 μM and 25μM catechol concentration using GE/β-CD-AuNPs/Tyr nanobiosensor (Fig. 5 inset). A steady-state response for catechol was obtained after 25 μM catechol (Fig. 5A) with the equation of $y = 0.1466x - 0.2417$ ($R^2 = 0.997$). Different concentrations of catechol responses using GE/β-CD-AuNPs /Tyr nanobiosensor are shown in Fig. 5B. Moreover, for analytical figures of merits, the values of the limit of detection (LOD) and limit of quantification (LOQ) were considered using the 3 s/m and 10 s/m (where "s" refers to the standard deviation, "m" refers to the slope of the calibration), respectively. Hence, LOD was calculated as 0.42 μM and LOQ as 1.26 μM. Moreover, the Lineweaver Burk was

Table 2
Comparison of GE/β-CD-AuNPs/Tyr nanobiosensor with different β-CD-AuNPs modified electrodes reported in the literature for various applications.

Biosensor	Analyte	Detection Method	Linear range	Detection limit	Application	Refs.
BSA/Ab/pβ-CD/ AuNPs/GC	prion protein	Impedance	15 fM to 1500 fM	2.1 fM	human blood serum	[29]
SH- β -CD/ AuNPs/ GO/GCE	tetrabromobisphenol A	Differential pulse voltammetry	1.5×10^{-8} to 7×10^{-6} M	1.2×10^{-9} M	water	[11]
AuNPs/CD–Fc/GOD	glucose	Amperometry	0.08–11.5 mM	15μM	Human plasma	[14]
Au/NF/CD/AuNPs	dopamine	Differential pulse voltammetry	0.05 − 280 μM	0.6 nM	urine	[49]
β-CD-capped AuNPs	cholesterol	Spectroscopic	5 aM to 0.5 μM	5 aM	human serum	[15]
SH-β-CD/AuNPs/rGO	acetaminophen	Differential pulse voltammetry	0.05–100 μM	0.03 μM	pharmaceutical formulations and human urine	[32]
	Ofloxacin		0.01–10 μM	0.008 μM		
β-CD- AuNPs	cysteine	Colorimetric	2.50 to 45.00 $\times 10^{-7}$ M.	25.47 $\times 10^{-9}$ M	human urine and blood serum	[50]
Au-CMCD/PCMCD	glucose	Amperometry	0.001−110 mM	0.99 μM	İnjection samples	[31]
Tβ-CD-Au NPs	naproxen	Colorimetric	4–180 μg L^{-1}	0.6 μg L^{-1}	Tablets wastewater and urine samples	[51]
NR-β-CD@AuNPs	NO_2^- ions	Fluorescence	0.0–0.9 μg.mL^{-1}	5.78 $\times 10^{-3}$ μg·mL^{-1}	water samples	[37]
AuNPs/SH-β-CD-GR/ GCE	Nonylphenol	Amperometry	0.05–50 μmol L^{-1}	0.017μM	Industrial wastewater, canal water	[30]
β -CD@AuNCs	dopamine	Fluorescence	100.0 nM- 80.0 μM	20.0 nM	human serum plasma and injection dosage forms	[52]
β-CD-AuNPs/GCE	NO_2^- ions	Amperometry	0.04–1470 μM	14 nM	tap water, packaged drinking water, and meat samples	[53]
GE/β-CD-AuNPs/ Tyr	**Catechol**	**Amperometry**	**1.56- 25μM**	**0.42 μM**	**Drug Inhibition**	**This work**

Fc: Ferrocene; NF: Nafion; NR: neutral red; PCA: pyrrole-2-carboxylic acid; PCMCD: carboxymethyl-β-cyclodextrin; PD: 1,10-phenanthroline-5,6-dione; poly(pyrrole-2-carboxylic acid); PPCA: poly(1,10-phenanthroline-5,6-dione); Tβ-CD: thiolated β-cyclodextrin.

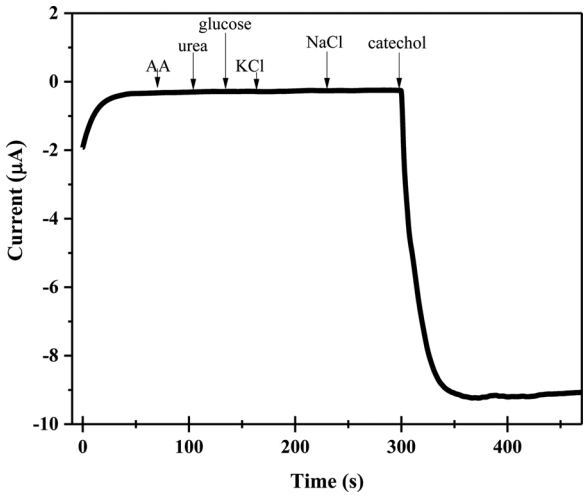

Fig. 6. Interference responses of GE/β-CD-AuNPs/Tyr nanobiosensor. Experimental conditions: 125 μM catechol and interferons at a working potential of −200 mV in 50 mM phosphate buffer at pH 7.0.

plotted to assess the enzyme kinetic studies, which was obtained from the calibration curve by plotting 1/I (μA^{-1}) *vs.*1/[S] (mM^{-1}). Using the Michaelis – Menten's relation: $1/I = 1/I_{max} + K_{mapp}/I_{max}$ [S], K_m and I_{max} values were calculated [27,28]. K_m was calculated as 27 μM and I_{max} as 1.70 μA, indicating that the substrate and enzyme relation is relatively low; hence, every enzyme-substrate complex results in a high K_m value. Moreover, the sensitivity value of the sensor was also estimated as 2.094 $\mu A.\mu M^{-1}. cm^{-2}$. One important aspect of the related study is that β-CD-AuNPs were produced via a one-step procedure. The product was applied for Tyr biosensor and IBU inhibition by an electrochemical method. The detailed literature comparison between GE/β-CD-AuNPs/Tyr nanobiosensor and different Tyr-based detection platforms for catechol is summarized in Table 1. Compared to our results with already published works reported in the literature, the proposed sensor shows remarkable sensor characteristics for catechol detection. The combination of β-CD and AuNPs serves as a great sensor platform for the Tyr enzyme and makes the sensor more targeted and effective than the pristine ones. Such combination not only provides a great microenvironment for enzyme immobilization but also facilitates the stabilization of AuNPs. Additionally, β-cyclodextrin capped AuNPs were promoted in the one-pot reaction without requiring extended stages as well as harsh conditions in biosensing applications. On the other hand, indirect strategies including sophisticated steps and multiple surface modifications of β-cyclodextrin/AuNPs were also conducted to fabricate CDs functionalize AuNPs [11,29–33].

Furthermore, various approaches on β-CD-AuNPs have been developed in order to improve the communication between the active site of the enzyme and electrode. Cosnier et al. designed a single-walled carbon nanotube framework with β-CD functionalized AuNPs, which encapsulated polymerized adamantine for glucose biosensor [34]. In their work, it was reported that the highest sensitivity and maximum current density were recorded for the configuration of β-CD functionalized AuNPs as an intermediate layer between adamantine-functionalized SWCNTs and

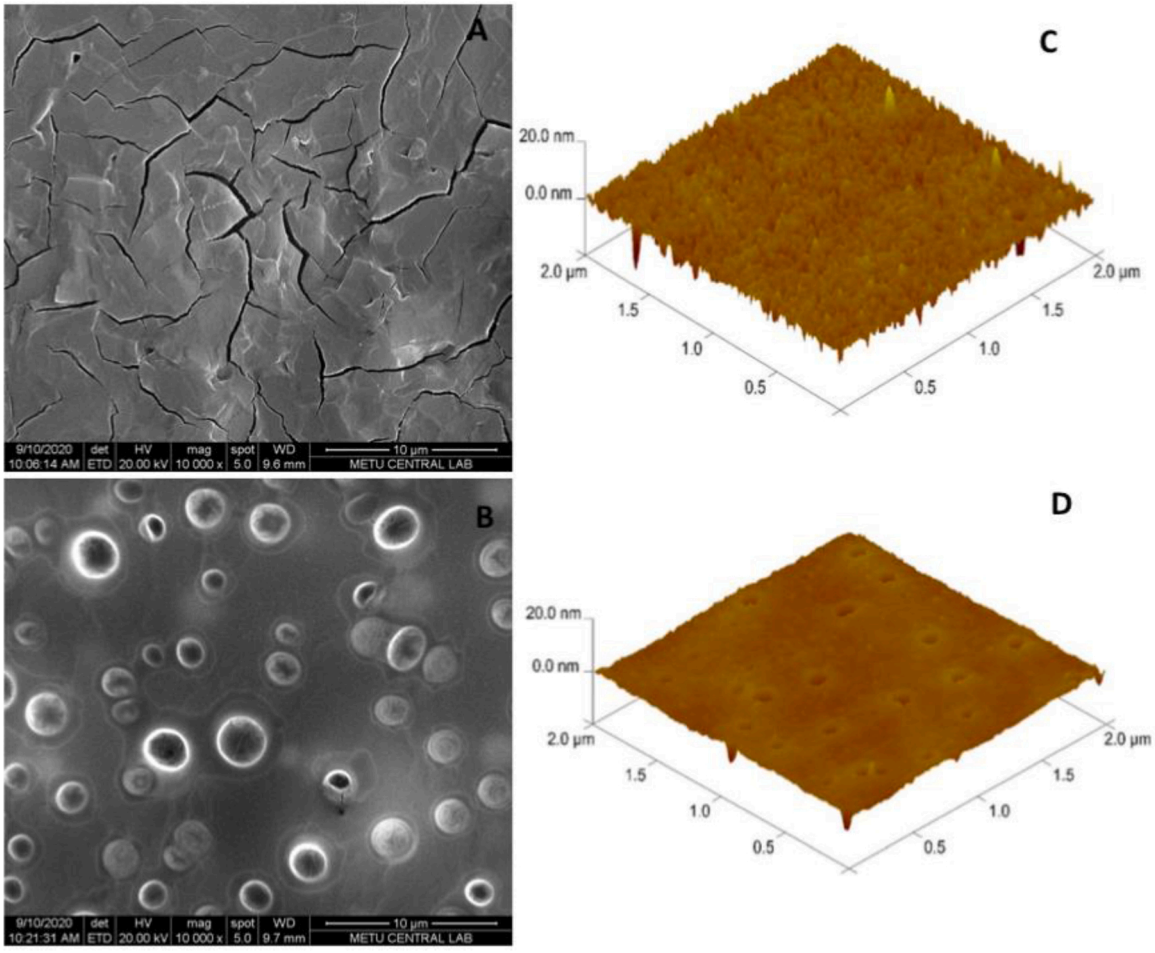

Fig. 7. Scanning electron microscopy images of synthesized β-CD-AuNPs (A) and (B) β-CD-AuNPs /Tyr and Atomic force microscopy images of synthesized β-CD-AuNPs (C) and β-CD-AuNPs /Tyr (D).

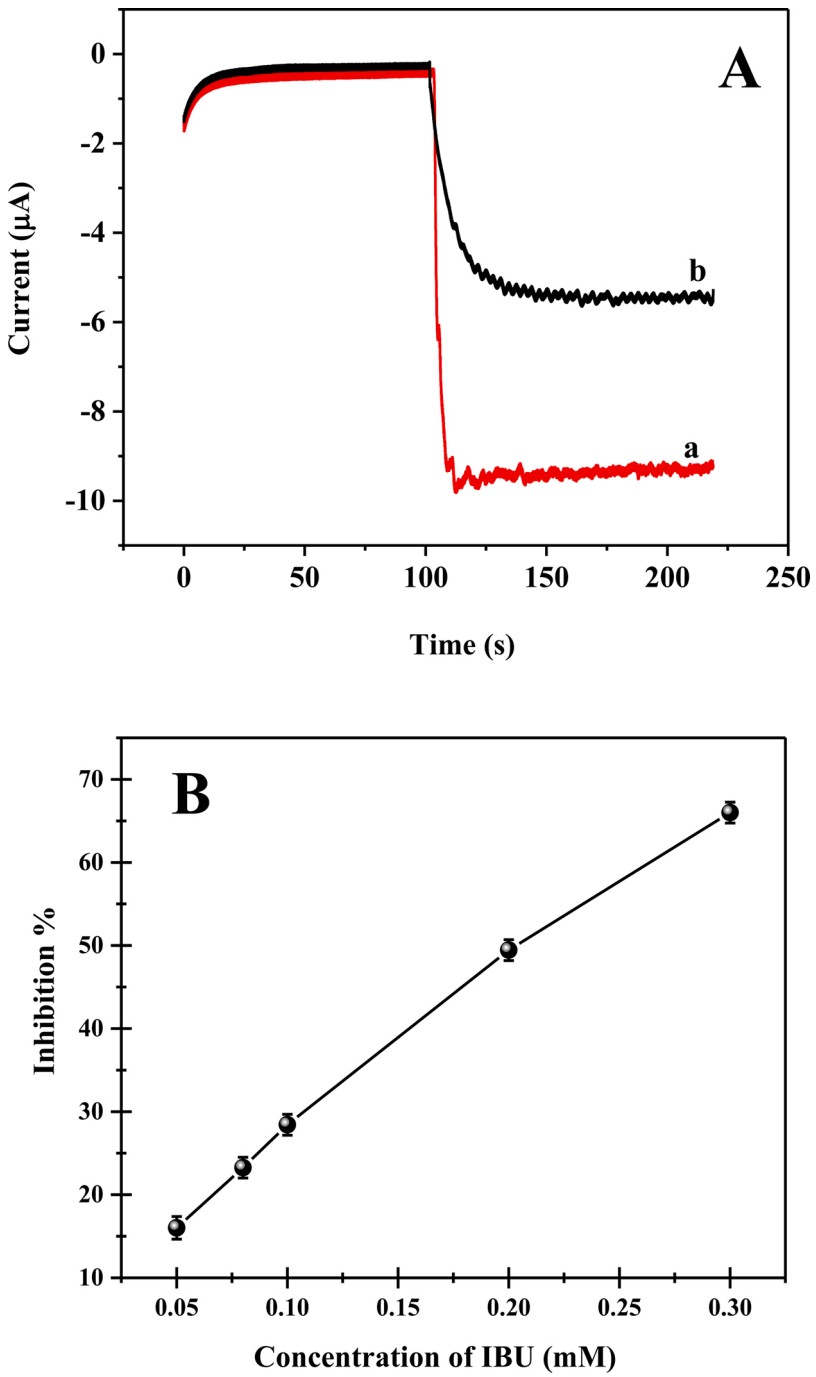

Fig. 8. (A) Current-time responses of GE/β-CD-AuNPs/Tyr nanobiosensor (a) before inhibition and (b) after 15 min inhibition with 100 μM IBU. Experimental conditions: 125 μM catechol at a working potential of −200 mV in 50 mM phosphate buffer at pH 7.0 (B) calibration curve using inhibition % *vs.* IBU concentration.

glucose oxidase. In another work, β-cyclodextrin capped AuNPs were suggested for the colorimetric analyses of dopamine, glucose, nabumetone [35,36], and trace analysis of nitrite [37]. The detailed comparison of GE/β-CD-AuNPs/Tyr nanobiosensor with different β-CD-AuNPs modified electrodes for various applications is also summarized in Table 2.

The suggested biosensor's performance was demonstrated by repeatability, reproducibility, shelf life, and interference experiments. Repeatability was examined by performing five runs adding 25 μM catechol in 50 mM phosphate buffer having a pH 7.0 using the same GE/β-CD-AuNPs/Tyr electrode. Besides, reproducibility was investigated by applying five independent measurements in different days in the same conditions using four similarly prepared GE/β-CD-AuNPs/Tyr electrodes. Low RSD values were obtained as 0.11 and 0.10 %, respectively, indicating a good repeatability (3.31 ± 0.34 μA) and reproducibility (3.02 ± 0.04 μA) of the sensor. Shelf life experiments were also performed by keeping the same biosensors at 4 °C for 25 days. At the end of the 10th day, the biosensors retained their 70 % activity.

Additionally, interference effects of commonly interfering ions and chemicals such as ascorbic acid, urea, glucose, KCl, and NaCl (125 μM each) were checked to verify their possible effect on biosensing response. As can be observed from Fig. 6, the suggested biosensor is selective to catechol in the presence of the commonly interfering ions and chemicals.

3.4. Surface morphologies of GE/β-CD-AuNPs /Tyr nanobiosensor

Homogeneity and surface characterization of the electrodes were examined by SEM and AFM studies. Fig. 7 (A–B) depicts SEM images of β-CD-AuNPs, and β-CD-AuNPs/Tyr modified electrodes. After biomolecule deposition, the surface morphology of the β-CD-AuNPs coated electrode changed considerably. As illustrated in Fig.7B, after the Tyr immobilization, surface was covered with Tyr homogenously and the protein molecules are well adhered onto this modified surface. After enzyme immobilization, the compact structure of the AuNPs bearing β-CD has been lost because of participation of functional groups in the cross-linking process and the obtained holes facilitate the diffusion of the substrate. Additionally, for investigating the surface topographies of the designed biosensor, AFM analyses were performed. Fig. 7 (C–D) display the AFM images of the surface morphology of β-CD-AuNPs and β-CD-AuNPs/Tyr modified surfaces. Within each modification step, the effect of modification can be clearly observed.

3.5. Inhibition effect of Ibuprofen on GE/β-CD-AuNPs /Tyr nanobiosensor

The characterized and optimized GE/β-CD-AuNPs /Tyr nanobiosensor was further used for the inhibition effect of IBU on Tyr activity (Fig. 8). The catechol responses before inhibition (I_o) and after inhibition (I) of Tyr by IBU current values were reported, and percent inhibition values were reported using the followed equation,

$$I\,\% = \frac{Io - I}{Io} \times 100 \quad (1)$$

The inhibition effect of IBU on Tyr was observed with different amounts of catechol response, incubation time (5−30 min), and IBU concentration (30–300 μM). Using the GE/β-CD-AuNPs /Tyr nanobiosensor, a 125 μM catechol response was monitored before and after the inhibition of Tyr (Fig. 8A). As nearly 25 % inhibition were observed in the presence of 100 μM IBU for 15 min incubation time, further studies were achieved using 15 min incubation time. In the linear range of 50 μM to 300 μM, with the equation of $y = 199.76x+7.4655$ ($r^2 = 0.995$). The inhibition effect of IBU was observed and reported as % inhibition *vs.* concentration of IBU (Fig. 8B). With the same figure of merit strategy in catechol detection, the inhibition effect of IBU was observed with the LOD value of 17 μM IBU and LOQ values of 50 μM. To understand the inhibition potential of a drug, I_{50} value should also be reported as a value at which 50 % inhibition was observed at a specific substrate concentration [38]. Hence, I_{50} value was calculated as 213 μM. Moreover, after inhibition studies, the I_{max} value decreased to 0.29 μA as a nature of inhibition kinetics; the inhibition process decreases the velocity of the enzymatic reactions. Hence, the K_m value was increased to 83 μM. In enzyme kinetics, for an irreversible inhibition mechanism, an incubation time is required since the reaction is time dependent. Moreover, once the inhibitors covalently bind to the enzymes, enzymes are permanently inactivated; hence I_{max} value decreases. In competitive inhibition mechanism, allosteric inhibitors bind at another place on the enzyme resulting in conformational changes in the active site where the substrate cannot bind. This results in an increase in the K_m value [39–43]. From this aspect, due to IBU effect on Tyrosinase-based nanobiosensor, the K_m value increased and the I_{max} value decreased, the inhibition mechanism can be suggested as a mixed type characteristic of enzyme kinetics. The inhibitor may bind both to the enzyme-substrate complex and the enzyme itself.

4. Conclusion

A novel electrochemical nanosensor based on the modification of a graphite electrode with β-CD-AuNPs/Tyr was fabricated. First, β-CD-AuNPs were synthesized, characterized, and used for biosensor construction. The sensor showed good biosensor characteristics for the determination of catechol compared to other studied electrodes (linear range of 1.56 μM-25 μM catechol concentration with LOD of 0.42 μM and sensitivity value of 2.094 μA. μM^{-1}. cm^{-2}). Later, the same sensor was evaluated for Tyr inhibition via IBU drug active compound through catechol response. According to the inhibition studies, using 15 min incubation time, I_{50} value was found to be 213 μM. To the best of our knowledge, this is the first study in the literature concerning both β-CD-AuNPs based Tyr biosensor and Tyr inhibition by IBU via an electrochemical method. The proposed sensor system with AuNPs and β-CD results in a conductive matrix formation, large surface area, and enhancement of the sensor's charge transferability. Furthermore, it is possible to discriminate catechol response from different interfering substances at appropriate experimental conditions, indicating a good selectivity of the sensor.

Declaration of Competing Interest

The authors report no declarations of interest.

Appendix A. Supplementary data

Supplementary material related to this article can be found, in the online version, at doi:https://doi.org/10.1016/j.procbio.2021.06.004.

References

[1] D.R. Thévenot, K. Toth, R.A. Durst, G.S. Wilson, Electrochemical biosensors: recommended definitions and classification, Biosens. Bioelectron. 16 (2001) 121–131, https://doi.org/10.1016/S0956-5663(01)00115-4.
[2] M. Gronow, Biosensors-a marriage of biochemistry and microelectronics, in: V. Moses, R.E. Cape (Eds.), Biotechnol. Sci. Bus., Harwood Academic Publishers, Amsterdam, 1991, pp. 335–370, https://doi.org/10.5860/choice.29-2705.
[3] L.D. Mello, L.T. Kubota, Review of the use of biosensors as analytical tools in the food and drink industries, Food Chem. 77 (2002) 237–256, https://doi.org/10.1016/S0308-8146(02)00104-8.
[4] S. Datta, L.R. Christena, Y.R.S. Rajaram, Enzyme immobilization: an overview on techniques and support materials, 3 Biotech 3 (2013) 1–9, https://doi.org/10.1007/s13205-012-0071-7.
[5] Z. Karim, M.J. Khan, M.Y. Maskat, R. Adnan, Immobilization of horseradish peroxidase on β-cyclodextrin-capped silver nanoparticles: its future aspects in biosensor application, Prep. Biochem. Biotechnol. 46 (2016) 321–327, https://doi.org/10.1080/10826068.2015.1031389.
[6] M. Holzinger, A. Le Goff, S. Cosnier, Nanomaterials for biosensing applications: a review, Front. Chem. 2 (2014) 1–10, https://doi.org/10.3389/fchem.2014.00063.
[7] P. Gopal, G. Narasimha, T.M. Reddy, Development, validation and enzyme kinetic evaluation of multi walled carbon nano tubes mediated tyrosinase based electrochemical biosensing platform for the voltammetric monitoring of epinephrine, Process Biochem. 92 (2020) 476–485, https://doi.org/10.1016/j.procbio.2020.02.006.
[8] C. Ozdemir, F. Yeni, D. Odaci, S. Timur, Electrochemical glucose biosensing by pyranose oxidase immobilized in gold nanoparticle-polyaniline/AgCl/gelatin nanocomposite matrix, Food Chem. 119 (2010) 380–385, https://doi.org/10.1016/j.foodchem.2009.05.087.
[9] N.A. Kalkan, S. Aksoy, E.A. Aksoy, N. Hasirci, Preparation of chitosan-coated magnetite nanoparticles and application for immobilization of laccase, J. Appl. Polym. Sci. 123 (2012) 707–716, https://doi.org/10.1002/app.34504.
[10] Q. Wang, L. Peng, G. Li, P. Zhang, D. Li, F. Huang, Q. Wei, Activity of laccase immobilized on TiO2-Montmorillonite Complexes, Int. J. Mol. Sci. 14 (2013) 12520–12532, https://doi.org/10.3390/ijms140612520.
[11] S. Luo, Y. Wu, Q. Mou, J. Li, X. Luo, A thio-β-cyclodextrin functionalized graphene/gold nanoparticle electrochemical sensor: a study of the size effect of the gold nanoparticles and the determination of tetrabromobisphenol A, RSC Adv. 9 (2019) 17897–17904, https://doi.org/10.1039/c9ra02614b.
[12] A. Kausaite-Minkstimiene, L. Glumbokaite, A. Ramanaviciene, A. Ramanavicius, Reagent-less amperometric glucose biosensor based on nanobiocomposite consisting of poly(1,10-phenanthroline-5,6-dione), poly(pyrrole-2-carboxylic acid), gold nanoparticles and glucose oxidase, Microchem. J. 154 (2020), 104665, https://doi.org/10.1016/j.microc.2020.104665.
[13] N. German, A. Popov, A. Ramanaviciene, A. Ramanavicius, Formation and electrochemical characterisation of enzyme-assisted formation of Polypyrrole and polyaniline nanocomposites with embedded glucose oxidase and gold nanoparticles, J. Electrochem. Soc. 167 (2020), 165501, https://doi.org/10.1149/1945-7111/abc9dc.
[14] M. Chen, G. Diao, Electrochemical study of mono-6-thio-β-cyclodextrin/ferrocene capped on gold nanoparticles: characterization and application to the design of glucose amperometric biosensor, Talanta. 80 (2009) 815–820, https://doi.org/10.1016/j.talanta.2009.07.068.

[15] N.M.Y. Zhang, M. Qi, Z. Wang, Z. Wang, M. Chen, K. Li, P. Shum, L. Wei, One-step synthesis of cyclodextrin-capped gold nanoparticles for ultra-sensitive and highly-integrated plasmonic biosensors, Sensors Actuators, B Chem. 286 (2019) 429–436, https://doi.org/10.1016/j.snb.2019.01.166.
[16] S. Soylemez, S.O. Hacioglu, M. Kesik, H. Unay, A. Cirpan, L. Toppare, A novel and effective surface design: conducting polymer/β-cyclodextrin host-guest system for cholesterol biosensor, ACS Appl. Mater. Interfaces 6 (2014) 18290–18300, https://doi.org/10.1021/am5054493.
[17] K.D. Rainsford, Ibuprofen: pharmacology, efficacy and safety, Inflammopharmacology 17 (2009) 275–342, https://doi.org/10.1007/s10787-009-0016-x.
[18] R. Bushra, N. Aslam, An overview of clinical pharmacology of ibuprofen, Oman Med. J. 25 (2010) 155–161, https://doi.org/10.5001/omj.2010.49.
[19] K. Sato, M. Toriyama, The inhibitory effect of non-steroidal anti-inflammatory drugs (NSAIDs) on the monophenolase and diphenolase activities of mushroom tyrosinase, Int. J. Mol. Sci. 12 (2011) 3998–4008, https://doi.org/10.3390/ijms12063998.
[20] A. Di Petrillo, A.M. González-Paramás, B. Era, R. Medda, F. Pintus, C. Santos-Buelga, A. Fais, Tyrosinase inhibition and antioxidant properties of Asphodelus microcarpus extracts, BMC Complement. Altern. Med. 16 (2016), https://doi.org/10.1186/s12906-016-1442-0.
[21] G. Mohiuddin, K.M. Khan, U. Salar, Kanwal, M.A. Lodhi, F. Begum, S. Perveen, Tyrosinase inhibitory activity of S-Naproxen derivatives, Lett. Drug Des. Discov. 16 (2019) 1276–1285, https://doi.org/10.2174/1570180816666190611162355.
[22] S. Pande, S.K. Ghosh, S. Praharaj, S. Panigrahi, S. Basu, S. Jana, A. Pal, T. Tsukuda, T. Pal, Synthesis of normal and inverted gold-silver core-shell architectures in β-cyclodextrin and their applications in SERS, J. Phys. Chem. C. 111 (2007) 10806–10813, https://doi.org/10.1021/jp0702393.
[23] T. Huang, F. Meng, L. Qi, Facile synthesis and one-dimensional assembly of cyclodextrin-capped gold nanoparticles and their applications in catalysis and surface-enhanced raman scattering, J. Phys. Chem. C. 113 (2009) 13636–13642, https://doi.org/10.1021/jp903405y.
[24] H.S.U. Kwo-Hsien, M.I.N.G. Hsueh-Yi, P.E.N.G. Kuen-Tung, H.U.A.N.G. Wei-Chin, Research on oscillopolarography I. Experimental verification of randles-sevcik equation, Acta Chim. Sin. (6) (1958) 3. https://en.cnki.com.cn/Article_en/CJFDTotal-HXXB195806003.htm.
[25] N.S. Neghmouche, T. Lanez, Calculation of electrochemical parameters starting from the polarization curves of ferrocene at glassy carbon electrode, Int. Lett. Chem. Phys. Astron. 4 (2013) 37–45. www.ilcpa.pl.
[26] N.S. Neghmouche, A. Khelef, T. Lanez, Electrochemistry characterization of ferrocene/ferricenium redox couple at glassycarbon electrode, J. Fundam. Appl. Sci. 1 (2) (2009) 23–30. http://www.jfas.info.
[27] T.C. Chou, P. Talalay, A simple generalized equation for the analysis of multiple inhibitions of Michaelis-Menten kinetic systems, J. Biol. Chem. 252 (1977) 6438–6442. http://www.jbc.org/.
[28] J.G. Wagner, Properties of the Michaelis-Menten equation and its integrated form which are useful in pharmacokinetics, J. Pharmacokinet. Biopharm. 1 (1973) 103–121, https://doi.org/10.1007/BF01059625.
[29] X. Li, J. Li, Y. Liu, X. Zhang, J. Chen, A sensitive electrochemical immunosensor for prion detection based on poly-B-cyclodextrin/gold nanoparticles/glassy carbon electrode, Sensors Actuators, B Chem. 250 (2017) 1–7, https://doi.org/10.1016/j.snb.2017.04.101.
[30] W. Chen, Y. Jiang, F. Xue, T. Zhang, Glassy carbon electrode modified with gold nanoparticles/thiol-β-cyclodextrin-graphene for the determination of nonylphenol, Int. J. Electrochem. Sci. 12 (2017) 12019–12036, https://doi.org/10.20964/2017.12.35.
[31] Y. Hui, X. Ma, F. Qu, F. Chen, J. Yu, Y. Gao, Electropolymerization of carboxymethyl-β-cyclodextrin based on co-electrodeposition gold nanoparticles electrode: electrocatalysis and nonenzymatic glucose sensing, J. Solid State Electrochem. 20 (2016) 1377–1389, https://doi.org/10.1007/s10008-016-3119-5.
[32] Z. Jiang, G. Li, M. Zhang, A novel electrochemical sensor based on SH-β-cyclodextrin functionalized gold nanoparticles/reduced-graphene oxide nanohybrids for ultrasensitive electrochemical sensing of acetaminophen and ofloxacin, Int. J. Electrochem. Sci. 12 (2017) 5157–5173, https://doi.org/10.20964/2017.06.28.
[33] Y. Shi, J. Goodisman, J.C. Dabrowiak, Cyclodextrin capped gold nanoparticles as a delivery vehicle for a prodrug of cisplatin, Inorg. Chem. 52 (2013) 9418–9426, https://doi.org/10.1021/ic400989v.
[34] M. Holzinger, L. Bouffier, R. Villalonga, S. Cosnier, Adamantane/β-cyclodextrin affinity biosensors based on single-walled carbon nanotubes, Biosens. Bioelectron. 24 (2009) 1128–1134, https://doi.org/10.1016/j.bios.2008.06.029.
[35] P.A. Nair, K. Sreenivasan, Non enzymatic colorimetric detection of glucose using cyanophenyl boronic acid included β-cyclodextrin stabilized gold nanoparticles, Anal. Methods 8 (2016) 2082–2087, https://doi.org/10.1039/c5ay02716k.
[36] J. Khodaveisi, S. Dadfarnia, A.M.H. Shabani, D. Saberi, Colorimetric determination of nabumetone based on localized surface plasmon resonance of functionalized gold nanoparticles as a chemical sensor, Sensors Actuators, B Chem. 239 (2017) 1300–1306, https://doi.org/10.1016/j.snb.2016.09.110.
[37] X. Du, X. Zhang, C. Jiang, W. Zhang, L. Yang, The trace detection of nitrite ions using neutral red functionalized SH-β-cyclodextrin @Au nanoparticles, Sensors (Switzerland). 18 (681) (2018) 1–12, https://doi.org/10.3390/s18030681.
[38] C. Yung-Chi, W.H. Prusoff, Relationship between the inhibition constant (KI) and the concentration of inhibitor which causes 50 per cent inhibition (I50) of an enzymatic reaction, Biochem. Pharmacol. 22 (1973) 3099–3108, https://doi.org/10.1016/0006-2952(73)90196-2.
[39] M.R. Roussel, S.J. Fraser, Global analysis of enzyme inhibition kinetics, J. Phys, Chem. 97 (1993) 8316–8327, https://doi.org/10.1021/j100133a031.
[40] N. Punekar, Enzymes: Catalysis, Kinetics and Mechanisms, Springer Nature, Singapore, 2018.
[41] L.R. Engelking, L.R. Engelking, Chapter 6 – enzyme kinetics. Textb. Vet. Physiol. Chem, 2015, pp. 32–38, https://doi.org/10.1016/B978-0-12-391909-0.50006-2.
[42] M.D. Luque de Castro, M.C. Herrera, Enzyme inhibition-based biosensors and biosensing systems: questionable analytical devices, Biosens. Bioelectron. 18 (2002) 279–294, https://doi.org/10.1016/S0956-5663(02)00175-6.
[43] J.V. Schloss, Significance of slow-binding enzyme inhibition and its relationship to reaction-intermediate analogues, Acc. Chem. Res. 21 (1988) 348–353, https://doi.org/10.1021/ar00153a005.
[44] S.A. Fathy, F.F. Abdel Hamid, A. El Nemr, A. El-Maghraby, E. Serag, Tyrosinase biosensor based on multiwall carbon nanotubes – titanium oxide nanocomposite for catechol determination, Desalin. Water Treat. 130 (2018) 98–108, https://doi.org/10.5004/dwt.2018.22847.
[45] C. Nistor, J. Emnéus, L. Gorton, A. Ciucu, Improved stability and altered selectivity of tyrosinase based graphite electrodes for detection of phenolic compounds. Anal. Chim. Acta, Elsevier, 1999, pp. 309–326, https://doi.org/10.1016/S0003-2670(99)00071-9.
[46] S. Sandeep, A.S. Santhosh, N.K. Swamy, G.S. Suresh, J.S. Melo, Detection of catechol using a biosensor based on biosynthesized silver nanoparticles and polyphenol oxidase enzymes, Port. Electrochim. Acta. 37 (2019) 257–270, https://doi.org/10.4152/pea.201904257.
[47] S.R. Yashas, S. Sandeep, B.P. Shivakumar, N.K. Swamy, Potentiometric polyphenol oxidase biosensor for sensitive determination of phenolic micropollutant in environmental samples, Environ. Sci. Pollut. Res. 27 (2020) 27234–27243, https://doi.org/10.1007/s11356-019-05495-2.
[48] S. Sandeep, A.S. Santhosh, N.K. Swamy, G.S. Suresh, J.S. Melo, N.A. Chamaraja, A biosensor based on a graphene nanoribbon/silver nanoparticle/polyphenol oxidase composite matrix on a graphite electrode: application in the analysis of catechol in green tea samples, New J. Chem. 42 (2018) 16620–16629, https://doi.org/10.1039/C8NJ02325E.
[49] N.F. Atta, A. Galal, D.M. El-Said, Novel design of a layered electrochemical dopamine sensor in real samples based on gold nanoparticles/β-Cyclodextrin/Nafion-Modified gold electrode, ACS Omega 4 (2019) 17947–17955, https://doi.org/10.1021/acsomega.9b01222.
[50] R. Rajamanikandan, A.D. Lakshmi, M. Ilanchelian, Smart phone assisted, rapid, simplistic, straightforward and sensitive biosensing of cysteine over other essential amino acids by β-cyclodextrin functionalized gold nanoparticles as a colorimetric probe, New J. Chem. 44 (2020) 12169–12177, https://doi.org/10.1039/d0nj02152k.
[51] J. Khodaveisi, A.M.H. Shabani, S. Dadfarnia, D. Saberi, A novel sensor for determination of naproxen based on change in localized surface plasmon peak of functionalized gold nanoparticles, Spectrochim. Acta - Part A Mol. Biomol. Spectrosc. 179 (2017) 11–16, https://doi.org/10.1016/j.saa.2017.02.008.
[52] M.I. Halawa, F. Wu, T.H. Fereja, B. Lou, G. Xu, One-pot green synthesis of supramolecular B-cyclodextrin functionalized gold nanoclusters and their application for highly selective and sensitive fluorescent detection of dopamine, Sensors Actuators, B Chem. 254 (2018) 1017–1024, https://doi.org/10.1016/j.snb.2017.07.201.
[53] P. Balasubramanian, T.S.T. Balamurugan, S.-M. Chen, Highly sensitive electrochemical detection of nitrite ions in food samples via β-Cyclodextrin capped gold nanoparticles film modified glassy carbon electrode, J. Electrochem. Soc. 164 (2017) B715–B722, https://doi.org/10.1149/2.1671713jes.